

# Photoelectrochemical Properties of Supramolecular Composite of Fullerene Nanoclusters and 9-Mesityl-10-carboxymethylacridinium Ion on SnO<sub>2</sub>

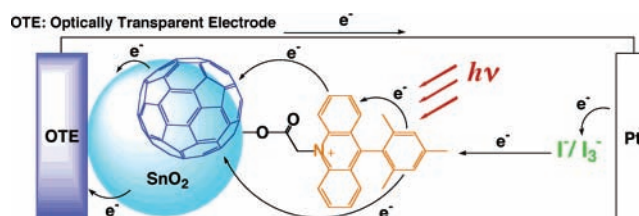
Taku Hasobe,<sup>†,‡</sup> Shigeki Hattori,<sup>†</sup> Hiroaki Kotani,<sup>†</sup> Kei Ohkubo,<sup>†</sup> Kohei Hosomizu,<sup>§</sup> Hiroshi Imahori,<sup>\*,§</sup> Prashant V. Kamat,<sup>\*,‡</sup> and Shunichi Fukuzumi<sup>\*,†</sup>

Department of Material and Life Science, Graduate School of Engineering, Osaka University, CREST, Japan Science and Technology Agency (JST), Suita, Osaka 565-0871, Japan, Radiation Laboratory and Department of Chemical & Biomolecular Engineering, University of Notre Dame, Notre Dame, Indiana 46556, and Department of Molecular Engineering, Graduate School of Engineering, Kyoto University, PRESTO, JST, Nishikyo-ku, Kyoto 615-8510, Japan

fukuzumi@ap.chem.eng.osaka-u.ac.jp; kamat@hertz.rad.nd.edu; imahori@scl.kyoto-u.ac.jp

Received June 10, 2004

## ABSTRACT



The photovoltaic cell composed of both fullerene nanoclusters and 9-mesityl-10-carboxymethylacridinium ion exhibits significant enhancement in the photoelectrochemical performance as well as broader photoresponse in the visible and near-infrared regions as compared with the reference system containing only each component.

Extensive efforts have so far been devoted to develop molecular triads, tetrad, pentads, etc., which can mimic a cascade of electron-transfer steps in the natural photosynthetic reaction center, leading to long-range charge separation with prolonged lifetime of the charge-separated state into second range.<sup>1–5</sup> However, the synthetic difficulty has precluded the development of low-cost photovoltaic devices using such molecular arrays.<sup>6–9</sup> In addition, a significant amount of energy is lost during the multistep electron-transfer

processes in both natural and artificial long-range charge separation. To avoid such wasted energy loss, we have

(2) (a) Wasielewski, M. R. *Chem. Rev.* **1992**, 92, 435. (b) Jordan, K. D.; Paddon-Row, M. N. *Chem. Rev.* **1992**, 92, 395. (c) Verhoeven, J. W. *Adv. Chem. Phys.* **1999**, 106, 603.

(3) Harriman, A.; Sauvage, J.-P. *Chem. Soc. Rev.* **1996**, 25, 41.

(4) (a) Fukuzumi, S.; Imahori, H. In *Electron Transfer in Chemistry*; Balzani, V., Ed.; Wiley-VCH: Weinheim, 2001; Vol. 2, pp 927–975. (b) Fukuzumi, S.; Guldi, D. M. In *Electron Transfer in Chemistry*; Balzani, V., Ed.; Wiley-VCH: Weinheim, 2001; Vol. 2, pp 270–337.

(5) (a) Imahori, H.; Guldi, D. M.; Tamaki, K.; Yoshida, Y.; Luo, C.; Sakata, Y.; Fukuzumi, S. *J. Am. Chem. Soc.* **2001**, 123, 6617. (b) Guldi, D. M.; Imahori, H.; Tamaki, K.; Kashiwagi, Y.; Yamada, H.; Sakata, Y.; Fukuzumi, S. *J. Phys. Chem. A* **2004**, 108, 541. (c) Gust, D.; Moore, T. A. In *The Porphyrin Handbook*; Kadish, K. M., Smith, K. M., Guillard, R., Eds.; Academic Press: San Diego, CA, 2000; Vol. 8, pp 153–190. (d) Gust, D.; Moore, T. A.; Moore, A. L. *Acc. Chem. Res.* **2001**, 34, 40.

<sup>†</sup> Osaka University.

<sup>‡</sup> University of Notre Dame.

<sup>§</sup> Kyoto University.

(1) Gust, D.; Moore, T. A.; Moore, A. L. In *Electron Transfer in Chemistry*; Balzani, V., Ed.; Wiley-VCH: Weinheim, 2001; Vol. 3, pp 272–336.



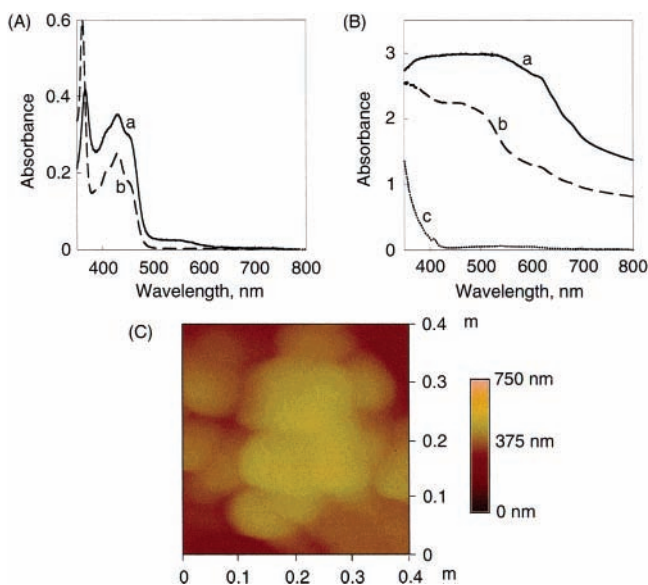


**Figure 1.** (A) Absorption spectra of (a) OTE/SnO<sub>2</sub>/Mes-Acr<sup>+</sup>-COOH and (b) Mes-Acr<sup>+</sup>-COOH in acetonitrile ( $4.0 \times 10^{-5}$  M). (B) Absorption spectra of (a) OTE/SnO<sub>2</sub>/Mes-Acr<sup>+</sup>-COOH + (C<sub>60</sub>)<sub>n</sub>, (b) OTE/SnO<sub>2</sub>/(C<sub>60</sub>)<sub>n</sub>, and (c) C<sub>60</sub> in toluene ( $1.5 \times 10^{-5}$  M). (C) AFM image of OTE/SnO<sub>2</sub>/Mes-Acr<sup>+</sup>-COOH + (C<sub>60</sub>)<sub>n</sub> electrode. [C<sub>60</sub>] = 0.62 mM in acetonitrile/toluene (3/1).

1C. The OTE/SnO<sub>2</sub>/Mes-Acr<sup>+</sup>-COOH + (C<sub>60</sub>)<sub>n</sub> film is composed of closely packed C<sub>60</sub> clusters of about 100 nm size, which renders a nanoporous morphology to the film. The grape bunch morphology of the cluster assembly thus provides a high surface area to the electrophoretically deposited film of C<sub>60</sub> clusters. As indicated earlier,<sup>14</sup> charging of fullerene moieties in the dc electric field plays an important role in the growth and deposition process. These films are quite robust and can be washed with organic solvents to remove any loosely bound C<sub>60</sub> nanoassemblies.

Photoelectrochemical measurements were performed using a standard two-electrode system consisting of a working electrode and a Pt wire gauze electrode in air-saturated acetonitrile containing 0.5 M NaI and 0.01 M I<sub>2</sub>. To evaluate the response toward the photocurrent generation, a series of photocurrent action spectra were recorded. The IPCE (incident photon-to-photocurrent efficiency) values were calculated by normalizing the photocurrent values for incident light energy and intensity and using the expression (1)<sup>15</sup>

$$\text{IPCE (\%)} = 100 \times 1240 \times i_{sc}/(I_{inc}\lambda) \quad (1)$$

where  $i_{sc}$  is the short circuit photocurrent (A/cm<sup>2</sup>),  $I_{inc}$  is the incident light intensity (W/cm<sup>2</sup>), and  $\lambda$  is the wavelength (nm). The maximum IPCE value of OTE/SnO<sub>2</sub>/Mes-Acr<sup>+</sup>-

(14) Kamat, P. V.; Barazzouk, S.; Thomas, K. G.; Hotchandani, S. J. *Phys. Chem. B* **2000**, *104*, 4014.

(15) Hasobe, T.; Imahori, H.; Fukuzumi, S.; Kamat, P. V. *J. Phys. Chem. B* **2003**, *107*, 12105.

COOH (spectrum a in Figure 2A) is only 2% (445 nm),

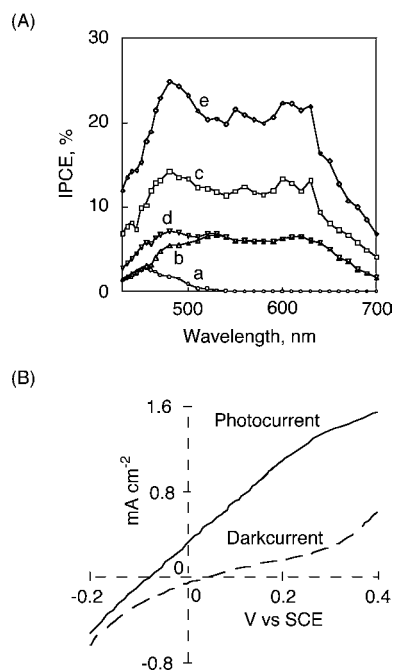


**Figure 2.** (A) Comparison of photocurrent response (IPCE values) of (a) OTE/SnO<sub>2</sub>/Mes-Acr<sup>+</sup>-COOH electrode ([C<sub>60</sub>] = 0.62 mM), (b) OTE/SnO<sub>2</sub>/(C<sub>60</sub>)<sub>n</sub> electrode ([C<sub>60</sub>] = 0.62 mM), (c) OTE/SnO<sub>2</sub>/Mes-Acr<sup>+</sup>-COOH + (C<sub>60</sub>)<sub>n</sub> electrode ([C<sub>60</sub>] = 0.62 mM), (d) the sum of the IPCE response of OTE/SnO<sub>2</sub>/Mes-Acr<sup>+</sup>-COOH and OTE/SnO<sub>2</sub>/(C<sub>60</sub>)<sub>n</sub> electrodes ([C<sub>60</sub>] = 0.62 mM), and (e) OTE/SnO<sub>2</sub>/Mes-Acr<sup>+</sup>-COOH + (C<sub>60</sub>)<sub>n</sub> electrode ([C<sub>60</sub>] = 0.62 mM) with applied bias potential: 0.2 V vs SCE. (B) I–V characteristics of OTE/SnO<sub>2</sub>/Mes-Acr<sup>+</sup>-COOH + (C<sub>60</sub>)<sub>n</sub> electrode ([C<sub>60</sub>] = 0.62 mM) under white light ( $\lambda > 370$  nm) illumination; electrolyte: 0.5 M NaI and 0.01 M I<sub>2</sub> in acetonitrile, input power: 28.3 mW/cm<sup>2</sup>.

whereas the IPCE value of OTE/SnO<sub>2</sub>/Mes-Acr<sup>+</sup>-COOH + (C<sub>60</sub>)<sub>n</sub> (spectrum c in Figure 2A) reaches 15% (480 nm).<sup>16</sup> On the other hand, the IPCE value of OTE/SnO<sub>2</sub>/Mes-Acr<sup>+</sup>-COOH + (C<sub>60</sub>)<sub>n</sub> is much higher than the sum of the two individual IPCE values of the individual systems (OTE/SnO<sub>2</sub>/Mes-Acr<sup>+</sup>-COOH and OTE/SnO<sub>2</sub>/(C<sub>60</sub>)<sub>n</sub>; spectrum d in Figure 2A) in the visible region.

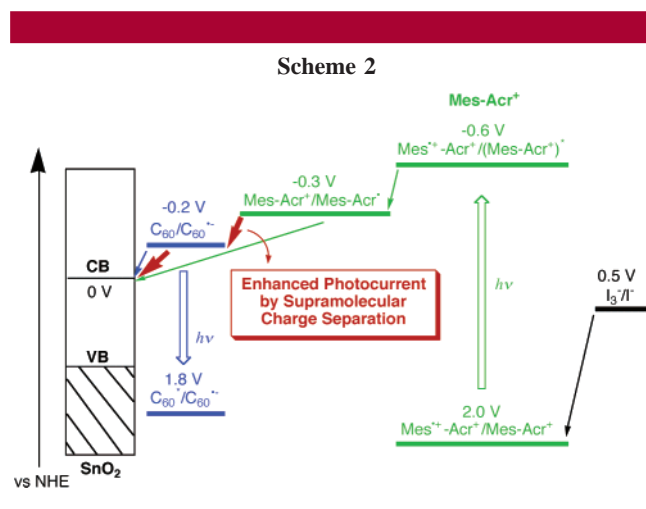
The charge separation in the OTE/SnO<sub>2</sub>/Mes-Acr<sup>+</sup>-COOH + (C<sub>60</sub>)<sub>n</sub> electrode can be further modulated by controlling the applied potential in a standard three-compartment cell as a working electrode along with a Pt wire gauze counter-electrode and a saturated calomel reference electrode (SCE).<sup>15</sup> Figure 2B shows I–V characteristics of the OTE/SnO<sub>2</sub>/Mes-Acr<sup>+</sup>-COOH + (C<sub>60</sub>)<sub>n</sub> electrode under the applied potential and is scanned toward more positive potentials. Increased charge separation and the facile transport of charge carriers under positive bias are responsible for enhanced photocurrent generation. At potentials greater than +0.4 V vs SCE, direct

(16) Overall power conversion efficiency ( $\eta$ ) of OTE/SnO<sub>2</sub>/Mes-Acr<sup>+</sup>-COOH + (C<sub>60</sub>)<sub>n</sub> electrode is estimated as 0.05% at input power ( $W_{in}$ ) of 28.3 mW cm<sup>-2</sup> ( $\lambda > 370$  nm); see the Supporting Information (S6).

electrochemical oxidation of iodide interferes with the photocurrent measurement. We evaluated the photocurrent action spectra of OTE/SnO<sub>2</sub>/Mes-Acr<sup>+</sup>-COOH + (C<sub>60</sub>)<sub>n</sub> under the electrochemical bias (spectrum e in Figure 2A). The maximum IPCE value is obtained as 25% at an applied potential of 0.2 V vs SCE. Such a high IPCE value indicates that photocurrent is initiated via electron-transfer between excited Mes-Acr<sup>+</sup>-COOH and C<sub>60</sub> clusters, followed by the charge transport to the collective surface of OTE/SnO<sub>2</sub> electrode. The charge transport is significantly improved under the influence of an applied bias.

To clarify the photocurrent generation mechanism, we examined formation of C<sub>60</sub> radical anion by nanosecond laser flash photolysis measurements. Time-resolved transient absorption spectra of 9-mesityl-10-methylacridinium ion without carboxylic acid (Mes-Acr<sup>+</sup>)<sup>10</sup> and fullerene in deoxygenated toluene–acetonitrile (1:1, v/v) have clearly exhibited a broad absorption band at about 1050 nm (see the Supporting Information).<sup>17,18</sup> This is diagnostic of the formation of the C<sub>60</sub> radical anion upon photoirradiation. Thus, electron transfer occurs from the acridinium radical moiety to C<sub>60</sub>, following photoinduced electron transfer from the mesitylene moiety to the singlet excited state of acridinium ion moiety of Mes-Acr<sup>+</sup>, to produce the electron-transfer state of Mes-Acr<sup>+</sup> dyad (Mes<sup>•+</sup>-Acr<sup>•</sup>), which has an extremely long lifetime. The absorption–time profile of the composite cluster (Mes-Acr<sup>+</sup> dyad and C<sub>60</sub>) in deoxygenated toluene–acetonitrile (1:1) recorded at 1050 nm was carried out (see the Supporting Information: S7). The second-order decay kinetics corresponds to electron transfer from the C<sub>60</sub><sup>•-</sup> to the Mes<sup>•+</sup> moiety, affording the second-order rate constant of back-electron transfer ( $k_{\text{bet}} = 2.9 \times 10^9 \text{ M}^{-1} \text{ s}^{-1}$ ).

The mechanism of the photocurrent generation of OTE/SnO<sub>2</sub>/Mes-Acr<sup>+</sup>-COOH and OTE/SnO<sub>2</sub>/Mes-Acr<sup>+</sup>-COOH + (C<sub>60</sub>)<sub>n</sub> electrodes is summarized in Scheme 2. In the case of



the OTE/SnO<sub>2</sub>/Mes-Acr<sup>+</sup>-COOH system, the photocurrent generation is initiated by photoinduced electron transfer in

Mes-Acr<sup>+</sup> dyad to produce Mes<sup>•+</sup>-Acr<sup>•</sup>. The reduced acridinium ion (Acr<sup>•</sup>) (Acr<sup>+</sup>/Acr<sup>•</sup> = -0.3 V vs NHE)<sup>10</sup> injects electrons into the conduction band of SnO<sub>2</sub> (0 V vs NHE),<sup>15</sup> whereas the oxidized mesityl moiety (Mes/Mes<sup>•+</sup> = 2.0 V vs NHE)<sup>10</sup> undergoes the electron-transfer reduction with the iodide (I<sub>3</sub><sup>-</sup>/I<sup>-</sup> = 0.5 V vs NHE)<sup>15</sup> in the electrolyte solution. On the other hand, in the case of the OTE/SnO<sub>2</sub>/Mes-Acr<sup>+</sup>-COOH + (C<sub>60</sub>)<sub>n</sub> electrode, the long lifetime of the electron-transfer state (Mes<sup>•+</sup>-Acr<sup>•</sup>) ensures efficient electron-transfer from Acr<sup>•</sup> to C<sub>60</sub> (C<sub>60</sub>/C<sub>60</sub><sup>•-</sup> = -0.2 V vs NHE)<sup>15</sup> to produce the C<sub>60</sub> radical anion (vide supra). While the reduced C<sub>60</sub> clusters inject electrons into the conduction band of SnO<sub>2</sub>, the oxidized mesityl moiety (Mes<sup>•+</sup>) undergoes the electron-transfer reduction with iodide ion in the electrolyte. Enhanced IPCE values of OTE/SnO<sub>2</sub>/Mes-Acr<sup>+</sup>-COOH + (C<sub>60</sub>)<sub>n</sub> (spectrum c in Figure 2A), relative to the sum of the two individual IPCE values of the individual systems (spectrum d in Figure 2A), may result from charge-transfer interaction between the mesityl (donor) moiety of Mes-Acr<sup>+</sup>-COOH and C<sub>60</sub> clusters, which appears at the long wavelength region over 500 nm.

In summary, we have constructed supramolecular photovoltaic cells using molecular nanocluster assemblies of fullerene and a simple molecular dyad (Mes-Acr<sup>+</sup>) with an extremely long lifetime and a high energy of the electron-transfer state. Remarkable improvement in the photoelectrochemical properties of the composite of Mes-Acr<sup>+</sup> dyad and fullerene nanoclusters has been achieved as compared with each component systems (OTE/SnO<sub>2</sub>/(C<sub>60</sub>)<sub>n</sub> and OTE/SnO<sub>2</sub>/Mes-Acr<sup>+</sup>-COOH), due to the extremely long lifetime of the electron-transfer state of Mes-Acr<sup>+</sup>-COOH and efficient electron transfer from Acr<sup>•</sup> to C<sub>60</sub>, together with the charge-transfer interaction between the mesityl (donor) moiety of Mes-Acr<sup>+</sup>-COOH and C<sub>60</sub> clusters.

**Acknowledgment.** This work was partially supported by a Grant-in-Aid from the Ministry of Education, Culture, Sports, Science and Technology, Japan. P.V.K. acknowledges support from the Office of Basic Energy Science of the U.S. Department of Energy. This is Contribution No. NDRL 4539 from the Notre Dame Radiation Laboratory and from Osaka University.

**Supporting Information Available:** Experimental Section (S1–S4), charge-transfer (CT) absorption spectrum of Mes-Acr<sup>+</sup> with C<sub>60</sub> (S5), and current–voltage characteristics of OTE/SnO<sub>2</sub>/Mes-Acr<sup>+</sup>-COOH + (C<sub>60</sub>)<sub>n</sub> (S6), and transient absorption spectra of Mes-Acr<sup>+</sup> with C<sub>60</sub> and the decay profile of absorbance at 1050 nm (S7). This material is available free of charge via the Internet at <http://pubs.acs.org>.

OL048913B

(17) Thomas, K. G.; Biju, V.; Guldi, D. M.; Kamat, P. V.; George, M. V. *J. Phys. Chem. B* **1999**, *103*, 8864.

(18) The extinction coefficient of C<sub>60</sub><sup>•-</sup> has been reported as 12000 M<sup>-1</sup> cm<sup>-1</sup>. See: Lawson, D. R.; Feldheim, D. L.; Foss, C. A.; Dorhout, P. K.; Elliot, C. M.; Martin, C. R.; Parkinson, B. *J. Electrochem. Soc.* **1992**, *139*, L68.